Current Biology, Volume *24*

Supplemental Information

Cdk1 Inactivation Terminates Mitotic Checkpoint Surveillance and Stabilizes Kinetochore Attachments in Anaphase

María Dolores Vázquez-Novelle, Laurent Sansregret, Amalie E. Dick, Christopher A. Smith, Andrew D. McAinsh, Daniel W. Gerlich, and Mark Petronczki

Supplemental Figures

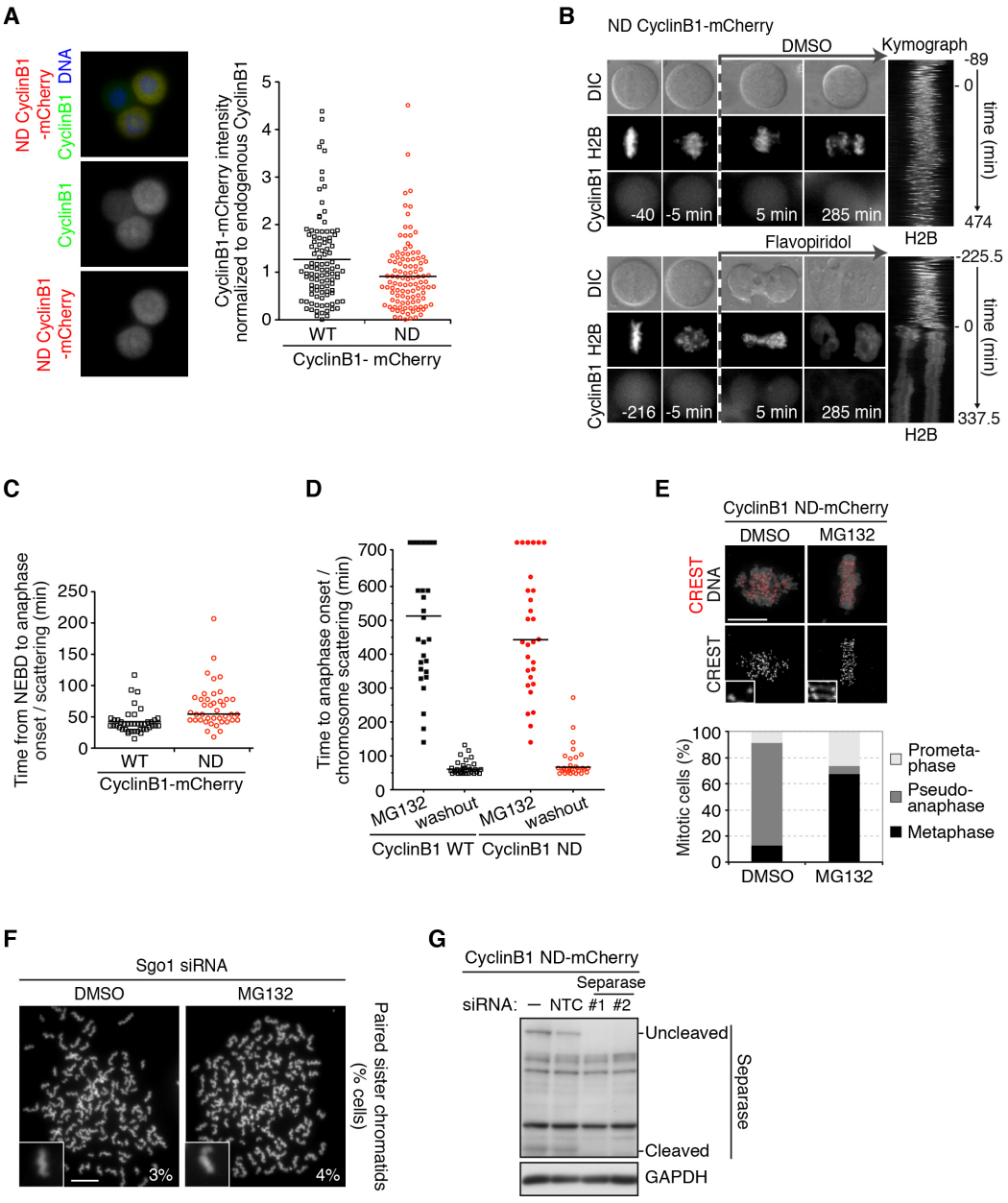

Figure S1 (Related to Figure 1). Expression of moderate levels of ND cyclin B1-mCherry causes proteolysis-dependent chromosome scattering and a Cdk activity-dependent mitotic arrest

(A) Levels of transgenic cyclin B1-mCherry (WT or ND) and endogenous cyclin B1 were measured by IF in cells arrested in prometaphase by addition of nocodazole (50 ng/ml) (n>101 cells). Cyclin B1-mCherry levels in transfected cells were normalized to the mean level of endogenous cyclin B1 in mitotic cells and are shown in a scatter plot (right). Horizontal black lines in the scatter plot represent the mean value.

(B) Time-lapse series and kymograph of cells expressing ND cyclin B1-mCherry that were treated at t = 0 min with flavopiridol or DMSO (control). 100% of cells treated with flavopiridol exited mitosis in comparison with 0% of control cells (n>5 cells).
(C) Timing of anaphase onset or chromosome scattering separation in cells expressing WT or ND cyclin B1-mCherry, respectively. The graph displays the time from NEBD to the anaphase onset or chromosome scattering (n>40 cells, in 3 independent experiments). Black lines in the dot plot mark the median.
(D) Analysis of time-lapse series of H2B-EGFP HeLa cells expressing WT or ND cyclin B1-mCherry that were arrested in metaphase (MG132 for 2 h) and subsequently (t = 0 min) released into anaphase/pseudo-anaphase, or kept in presence of MG132 (n>29). Horizontal black lines represent median in the scatter dot plot.
(E) IF analysis of centromeres in mitotic cells expressing ND cyclin B1-mCherry (n>299 cells from 3 independent experiments). Cells were synchronously released into mitosis and then treated with DMSO (control) or MG132 for 4 hours.
(F) Chromosome spread analysis of cells transfected with Sgo1 siRNA. Cells were synchronously released into mitosis and treated with DMSO (control) or MG132 for 4 hours (n>299 spreads from 3 independent experiments). Scale bars represent 10μm.
(G) Immunoblot analysis of protein extracts prepared from nocodazole-arrested cells expressing ND cyclin B1-mCherry that were transfected with NTC siRNA or siRNA duplexes targeting separase.

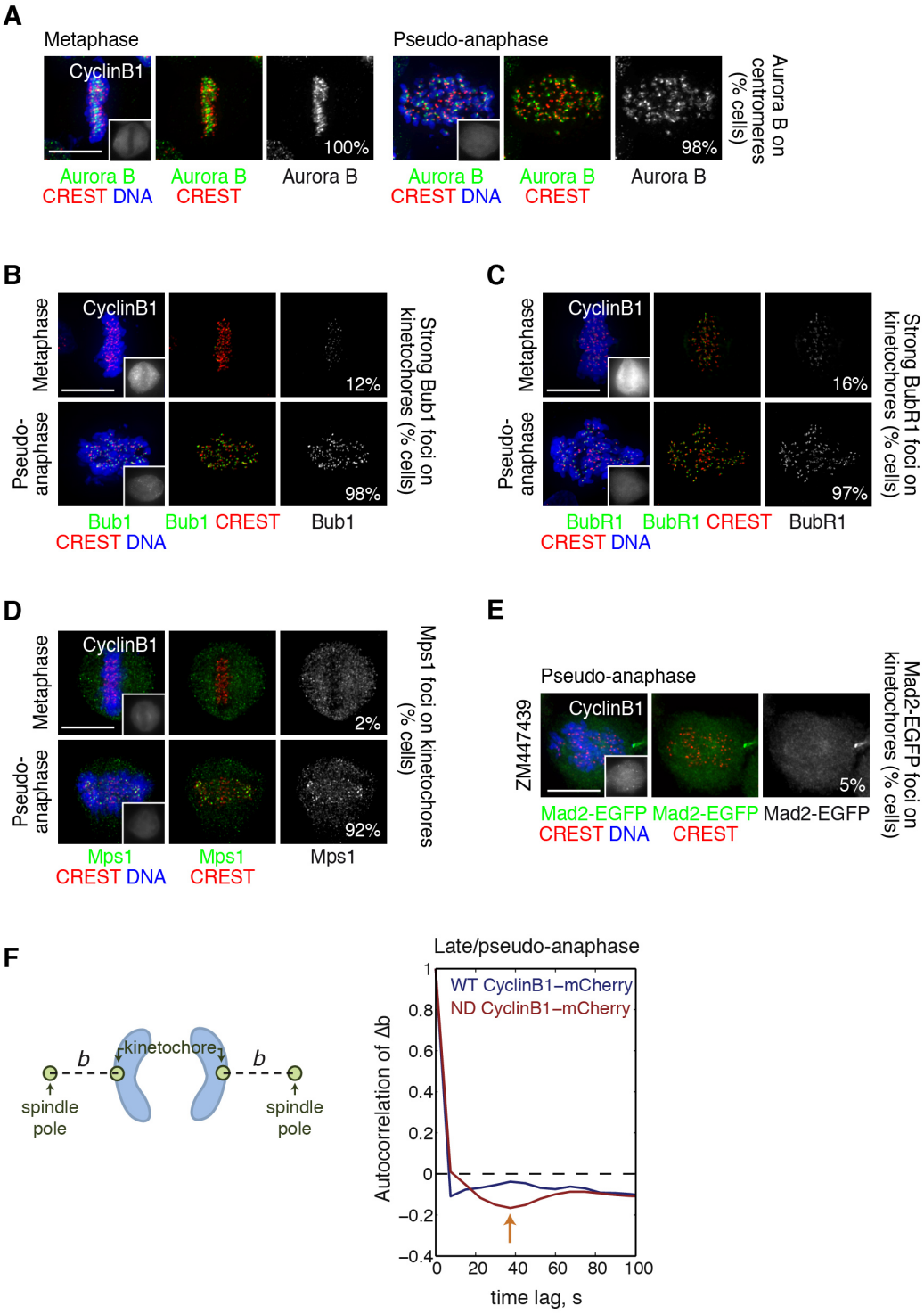

Figure S2 (Related to Figure 2). Kinetochore recruitment of mitotic checkpoint proteins and oscillatory kinetochore movements in pseudo-anaphase cells

(A) IF analysis of Aurora B, (B) Bub1, (C) BubR1 and (D) Mps1 localization in metaphase and pseudo-anaphase cells expressing ND cyclin B1-mCherry (n>149 cells from 3 independent experiments).

(E) Mad2 localization was analyzed by IF 2 h after MG132 release in cells expressing ND cyclin B1-mCherry. Aurora B kinase inhibitor ZM447439 (2 μM) [S1] was added

40 min after release from MG132 arrest (n>149 cells from 3 independent experiments). Scale bars represent 10 µm.
(F) Autocorrelation analysis [S2] of the change in distance b (see schematic) over time for late anaphase (WT cyclin B1; n=21) and pseudo-anaphase cells (ND cyclin B1; n=30). Half-period of oscillation is indicated by orange arrow. Autocorrelation analysis of the spindle pole-to-kinetochore distance over time, confirmed that there is oscillatory motion in pseudo-anaphase compared to normal late anaphase.

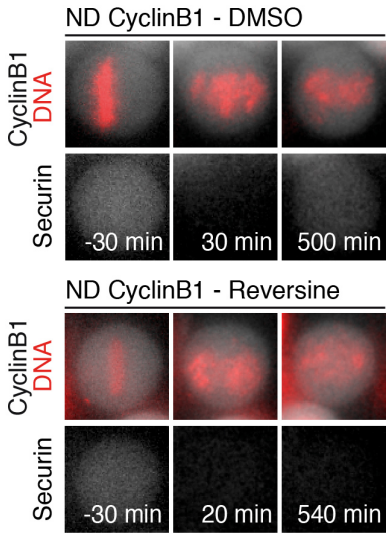

Figure S3 (Related to Figure 3). Securin-EGFP accumulation in pseudo-anaphase cells depends on Mps1 kinase activity
Frames of live-cell imaging of HeLa cells stained with Hoechst 33342 expressing securin-EGFP and ND cyclin B1-mCherry are shown. 1 h after release from nocodazole (30 ng/ml) cells expressing ND cyclin B1 were treated with DMSO or reversine (0.5 µM).

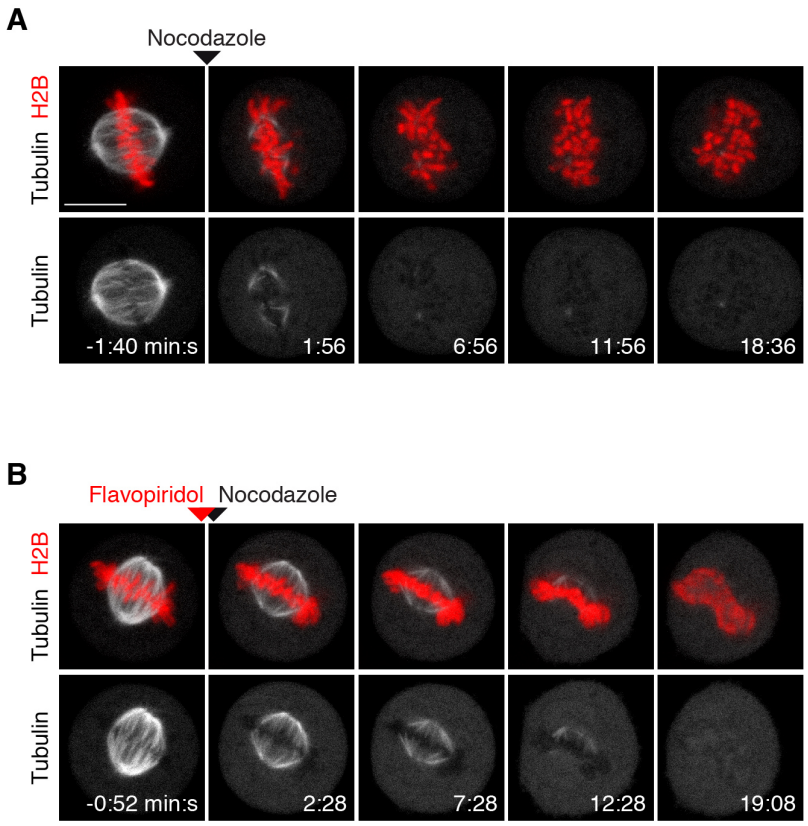

Figure S4 (Related to Figure 4). Kinetics of spindle depolymerization upon acute flavopiridol and nocodazole treatment

HeLa cells expressing H2B-mCherry and mEGFP-α-tubulin were arrested in metaphase with MG132 and imaged by 3D-confocal live-cell microscopy. Nocodazole (1 µg/ml) and flavopiridol (20 µM) were added acutely during imaging as indicated by the arrowheads. Images show single confocal z sections of representative cells. Time = 0:00 min:sec at the first drug addition.

(A) Spindle depolymerization upon nocodazole addition.

(B) Spindle depolymerization upon flavopiridol and nocodazole addition. Cells were acutely treated for 100 sec with flavopiridol prior to nocodazole addition. Scale bars, 10 µm.

Supplemental Experimental Procedures

Cell Culture, Synchronization and Drug Treatment

HeLa Kyoto, HeLa H2B-EGFP and HEK 293FT cells were grown as described in [S3]. HeLa Mad2-EGFP cells (a kind gift by Tony Hyman) [S4] were grown in medium supplemented with 500 μg/ml G418. HeLa GFP-CENPA (kindly gifted by P. Lenart [S5, 6]) were grown in medium supplemented with 0.4 μg/ml puromycin. Medium containing 200 μg/ml hygromycin B was used to grow HeLa H2B-iRFP (kind gift from K.C. Su). HeLa Mad2-EGFP H2B-iRFP cells were grown in medium supplemented with 500 μg/ml G418 and 200 μg/ml hygromycin B. HeLa Kyoto H2B-mCherry Mad2-EGFP monoclonal cells were described previously [S7] and grown in medium supplemented with 500 μg/ml G418 and 0.5μg/ml puromycin. Medium containing 300 μg/ml G418 and 0.3 μg/ml puromycin was used for growth of HeLa Kyoto EGFP-CENP-A EGFP-Centrin1 cells as previously described [S8]. For all the experiments (except Figures 4 and S4) cells were arrested for 20-22 h with 2 or 2.5 mM thymidine and subsequently synchronously released into mitosis for 8 to 17 h. For Figure 3B, 8 h after release a second thymidine arrest was performed and cells were subsequently synchronized at the metaphase-to-anaphase transition using a nocodazole-MG132 protocol according to [S3]. Drug concentrations used were 10 μM MG132 (Sigma), 15 μM flavopiridol (except in Figures 4B and S4, 20 μM flavopiridol) (Sigma), 100 nM BI 2536 [S6], 30 ng/ml nocodazole (Sigma) (Figures 3D and S3), 50 ng/ml nocodazole (Figures 3B, 3C, S1A and S1G), 1 μg/ml nocodazole (Figures 4 and S4), and 0.5 μM reversine (Sigma) [S9], and 2 μM ZM447439 (Tocris Bioscience) [S1].

siRNA Depletion, Plasmid Transfection and Lentivirus Infection.

The following siRNA duplexes were transfected at a final concentration of 20 nM using Lipofectamine RNAiMax (Invitrogen): Non targeting control (NTC, negative universal control siRNA medium GC), separase #1 (Thermo Scientific siGENOME D004104-01), separase #2 (Invitrogen Stealth HSS114543), Sgo1 (Invitrogen Stealth HSS135742). siRNA duplexes were transfected into cycling cells 24 hours prior to plasmid transfection and synchronization with thymidine (Sigma) (Figures 1E and S1G) or immediately prior to thymidine treatment (Figures 1C and S1F). Cycling cells were transfected using FuGene HD (Roche) with plasmids for expression of cyclin B1-mCherry WT (wild type) or ND (non-degradable, carrying the two D-box motif point mutations R42A and L45A) (kindly provided by J. Pines [S10]) (Figures 1, 2, 3A-C, S1 and S2) or in which the first 87 amino acids have been deleted Δ87-cyclin B1 (Figures 3D and S3), and pIRES-securin-EGFP [S11] (Addgene, 26464) (Figures 1D, 3A, 3D and S3) just prior to synchronization with thymidine. Transfection efficiency of ND cyclin B1-mCherry was determined for experiments in Figures 1B, 1C and 2D. More than 70% of mitotic cells were expressing the transgenic proteins 17 h after thymidine release and more than 50% of MG132-treated mitotic cells were transgene-positive (n>200 mitotic cells in each experiment). Viral particles were collected at 24 and 48 h after HEK 293FT cells were transfected with pLVX-IRES-Puro-cyclin B1-mCherry (WT or ND) and the two second generation packaging system plasmids psPAX2

(Addgene, 12260) and pMD2.G (Addgene, 12259) using Lipofectamine 2000 (Invitrogen). HeLa Kyoto cells were infected with lentiviral particles in presence of 8 μg/ml polybrene (Sigma) 30 minutes after released from the first thymidine block. Infection efficiency was determined after nocodazole treatment for WT cyclin B1-mCherry (>89%) and for ND cyclin B1-mCherry (>60%) (n>207 cells in each experiment) (Figure 3B and 3C).

Antibodies, dyes and FISH probes

Primary antibodies used for immunofluorescence were mouse monoclonal anti-α-tubulin (B512, Sigma, 1:500), rabbit polyclonal anti-Aurora B (ab2254, Abcam, 1:500), mouse monoclonal anti-Bub1 (clone 4H5, MBL International, 1:200), sheep anti-BubR1 (kindly provided by S. Taylor [S12], 1:1000), human CREST anti-centromere (HCT-0100, Immunovision, 1:1000), mouse monoclonal anti-cyclin B1 (GNS1, Sc-245 Santa Cruz Biotechnology, 1:400), rabbit anti-cyclin B1 (H-433, Sc-752, Santa Cruz Biotechnology, 1:500), mouse monoclonal anti-GFP (clones 7.1 and 13.1, Roche, 1:1000), mouse monoclonal anti-mCherry (632543, Living Colors, 1:1000), mouse monoclonal anti-Mps1 (clone N1, Invitrogen, 1:500), rat monoclonal anti-RFP (5F8, Chromotek, 1:400) and Alexa 488-conjugated mouse monoclonal anti-Mad1 (clone BB3-8, kindly provided by A. Musacchio [S13], 1:600). Cross-adsorbed secondary antibodies conjugated to Alexa 488, Alexa 594, Alexa 568 or Alexa 647 (Molecular Probes, Invitrogen) were used for detection. EGFP was detected in fixed cells using GFP-booster_Atto488 (Chromotek). DNA staining in fixed and living cells was performed using 1 μg/ml DAPI and 1 μM Hoechst 33342, respectively (Molecular Probes). Primary antibodies used for immunoblotting were mouse monoclonal anti-Cdc20 (clone BG1.3, kindly provided by Julian Gannon), mouse monoclonal anti-cyclin B1 (GNS1, Sc-245 Santa Cruz Biotechnology, 1:1000), mouse monoclonal anti-GAPDH (clone 6C5, ab8245, Abcam, 1:50,000), mouse monoclonal anti-Mad2 (610678, BD Transduction Laboratories, 1:500), rabbit polyclonal anti-Mad2 (A300-301A, Bethyl laboratories, 1:1000), mouse monoclonal anti-securin (DCS-280, ab3305, Abcam, 1:500) and mouse monoclonal anti-separase (XJ11-1B12, ab16170, Abcam, 1:200). Goat Hrp-conjugated secondary antibodies (GE Healthcare) were used for ECL detection and Dylight®-conjugated secondary antibodies for fluorescent immunoblotting (5257, anti-mouse IgG 800 and 5366, anti-rabbit IgG 680, Cell Signalling). Quantitative immunoblotting was analyzed on a LI-COR® Odyssey scanner. For MCC immunoprecipitation, mouse monoclonal anti-Cdc20 (p55 CDC H-7, Santa Cruz Biotechnology) was covalently coupled with Dynabeads® (Novex). For FISH (Fluorescence *in situ* hybridization), probes for the centromeres of chromosomes 6 (LPE 06G, Cytocell aquarius) and 8 (LPE 08R, Cytocell aquarius) were used.

Immunofluorescence

HeLa Kyoto and HeLa Mad2-EGFP were fixed with 4% formaldehyde at RT for 20 minutes and processed for immunofluorescence microscopy (IF) as described [S6]. The fixation solution was prepared in PBS (Figure S1A and S1E) or in PHEM buffer containing 0.2% Triton X-100 (Figures 2A, 2B and S2). Prior to fixation, 5 seconds pre-

extraction in PHEM containing 0.2% Triton X-100 was performed for Mps1 staining (Figure S2D). Cold treatment (cells were kept on ice for 20 minutes) and cold-resistant microtubule analysis were performed according to [S6] (Figure 2D).

Chromosome Spreads

Chromosome spreads of HeLa Kyoto cells were obtained by incubating mitotic cells in a hypotonic solution (DMEM:filtered deionized water at 1:2 ratio) for 6 min at room temperature (RT). Subsequently, cells were fixed with Carnoy's buffer (freshly made) for 15 min at RT and spun down, this fixation step was repeated four times. The suspension of cells in Carnoy's buffer (100 µl) is dropped on a clean slide from about 80 cm distance and let dry at RT. DAPI (1µg/ml) was added with the mounting solution (ProlongGold, Invitrogen) (Figures 1B and S1F).

Fluorescent *In Situ* Hybridization

Fluorescence *in situ* hybridization (FISH) was performed following Cytocell's instructions. Briefly, cells were grown on a coverslip and fixed with Carnoy's buffer (15 min at RT), washed with 2x SSC (saline sodium citrate), dehydrated in an ethanol series (70%, 80%, 100%) and air-dried. FISH probes (mixed with hybridization solution, provided by Cytocell aquarius) were added to a slide and the coverslip with cells was placed on top and sealed with rubber solution glue. Denaturation was performed for 2 min at 77^{o}C, and the slide was incubated overnight at 37^{o}C for hybridization in a humid and lightproof container. Subsequently, the coverslips were washed once in 0.25 x SSC for 2 min at 73^{o}C and twice in 2 x SSC with 0.05% Tween 20 for 30 sec at RT. Samples were mounted using ProlongGold (Invitrogen) with 1µg/ml DAPI (Figure 1C).

Microscopy of Fixed Samples

Images were acquired on a Zeiss Axio Imager M1 microscope using Plan Neofluor 40x/1.3 oil objective lens (Figures 2D quantification and S1A) and Plan Apochromat 63x/1.4 oil DIC objective lens (Zeiss) (Figures 1B, 1C, 1E, 2A, 2B, 2D, 4A, S1E, S1F, and S2) equipped with an ORCA-ER camera (Hamamatsu) and controlled by Volocity 5.5.1 software (Improvision). Images are displayed as maximum-intensity projections of deconvolved z planes (generated by Volocity's iterative restoration function) that were acquired in 0.1 µm sections (Figures 1C, 1E, 2A, 2B, 2D, 4A, S1E, and S2) or as a single plane (Figures 1B, S1A, S1F and mCherry images in Figures 2A, 2B and S2).

Live-Cell Imaging

Culture medium was changed to phenol-red-free CO_2-independent medium prior to start recording. Frames were acquired using an EC Plan Neofluor 40x/1.30 oil DICIII objective lens on an Axio Observer Z1 microscope (Zeiss) controlled by SimplePCI6 software equipped with a full-enclosure environmental chamber heated to 37^{o}C (Digital Pixel Imaging) and an ORCA 03GO1 camera (Hamamatsu) (Figures 1A, S1B, S3, and images for quantification in Figures 3A, 3D, S1C and S1D). Frames were recorded as three z planes (5µm apart) every 3 min (Figures 1A and S1C), every 3.5 min (Figure S1B), every 4 min (Figure 3A and Figure S1D, for image quantification) or every 10

min (Figure 3D and S3). Single z planes are displayed for DIC and cyclin B1-mCherry, whereas a maximum intensity projection is shown for H2B-GFP in Figures 1A, S1B and S3. For Figures 1D, 2C and 3A, frames were acquired as z planes (2.5 µm apart) every 6 min (Figures 1D and 3A, shown pictures) or as z planes (1 µm apart) every 5 min (Figure 2C) at 37°C using a Nikon TE2000 microscope equipped with a Plan Fluor 60x/1.4 DIC H lens (Nikon), a PerkinElmer ERS Spinning disk system, a CSU22 spinning disk scanner (Yokogawa), a IEEE 1394 Digital CCD C4742-80-12AG camera (Hamamatsu) and controlled by Volocity 6.0.1 software (Perkin Elmer). Images are displayed as maximum-intensity projections of central z planes. For Figure 2E, frames were acquired using a Nikon TiE microscope coupled with a Plan-Apochromat 100x/1.49 UV-C lens (Nikon), an UltraVIEW Vox system, CSU-X1-A3 spinning disk scanner (Yokogawa), a IEEE 1394b-2002 Digital CCD ORCA-R2 camera (Hamamatsu) and controlled by Volocity 6.1.2 software (Perkin Elmer); image stacks consisted of 25 z planes (0.5 µm apart) every 7.5 s imaged at 37°C. Tracking of EGFP-labelled CENP-A and Centrin1 was performed using the previously described Maki tracking software [S14]. Autocorrelation curves were calculated as previously described [S2]. For Figures 4B and S4, culture medium was changed to DMEM without phenol-red and riboflavin to reduce auto-fluorescence. 9 z planes (1.6 µm apart) were obtained by confocal live cell microscopy every 100 sec on a customized Zeiss LSM780 microscope using a 40x 1.4 N.A. Oil DIC Plan-Apochromat objective (Zeiss), controlled by ZEN 2011 software. The microscope was equipped with an EMBL incubation chamber (European Molecular Biology Laboratory), providing a humidified atmosphere at 37°C with 5% CO_2. Processing of images was performed using ImageJ64 1.43u and Fiji (ImageJ 1.48d) software [S15].

Image Quantification

For Figures 2D, 3A and 3D, α-tubulin, securin-EGFP and cyclin B1-mCherry integrated cellular intensities were measured and background corrected. In Figure S1A, the relative levels of cyclin B1-mCherry in each cell were calculated as follows: the mean cyclin B1 intensity of non-transfected cells (mCherry-negative) was subtracted from the mean cyclin B1 intensity of an individual transgene expressing cell (mCherry-positive). The resulting value was normalized to the mean cyclin B1 intensity of non-transfected cells (mCherry-negative) after background correction. All these measurements were performed in 16-bit single in-focus z plane images using ImageJ64 1.43u software. For Figure 4B, microscopy images were processed and analyzed using Fiji. Mad2-EGFP intensity in chromatin regions was measured in average intensity projections of the middle 6 z-sections. Chromatin regions were automatically determined in maximum intensity projections of the respective 6 z-sections using a Fiji macro: images were converted using a HiLo lookup table, then the threshold was auto-adjusted with "method=Moments white" and finally a selection at the respective area was created. To calculate Mad2-EGFP increase over cytoplasm the cytoplasmic EGFP background and image background were measured in Mad2-EGFP average intensity projections.

Immunoprecipitation

HeLa Kyoto cells infected and synchronized in mitosis as indicated before were lysed in Buffer A (50 mM Tris pH 8.0, 150 mM NaCl, 0.5% NP-40, 1 mM DTT, 1 µM okadaic acid, 1 µM MC-LR and a protease inhibitor tablet from Roche). Protein concentrations were adjusted to 4.8 mg/ml and 1.2 mg lysates were incubated with 15 µl Dynabeads® Protein A magnetic beads (Novex) coupled to Cdc20 antibodies for 1h at 4°C. After 3 washes in buffer A, proteins were eluted by incubating the beads in sample buffer for 10 minutes at 95°C. Proteins were finally resolved by SDS-PAGE and transferred to PVDF membranes.

Supplemental References

S1. Ditchfield, C., Johnson, V.L., Tighe, A., Ellston, R., Haworth, C., Johnson, T., Mortlock, A., Keen, N., and Taylor, S.S. (2003). Aurora B couples chromosome alignment with anaphase by targeting BubR1, Mad2, and Cenp-E to kinetochores. J. Cell Biol. *161*, 267-280.

S2. Vladimirou, E., McHedlishvili, N., Gasic, I., Armond, J.W., Samora, C.P., Meraldi, P., and McAinsh, A.D. (2013). Nonautonomous movement of chromosomes in mitosis. Dev. Cell *27*, 60-71.

S3. Petronczki, M., Glotzer, M., Kraut, N., and Peters, J.M. (2007). Polo-like kinase 1 triggers the initiation of cytokinesis in human cells by promoting recruitment of the RhoGEF Ect2 to the central spindle. Dev. Cell *12*, 713-725.

S4. Hutchins, J.R., Toyoda, Y., Hegemann, B., Poser, I., Heriche, J.K., Sykora, M.M., Augsburg, M., Hudecz, O., Buschhorn, B.A., Bulkescher, J., et al. (2010). Systematic analysis of human protein complexes identifies chromosome segregation proteins. Science *328*, 593-599.

S5. Kunitoku, N., Sasayama, T., Marumoto, T., Zhang, D., Honda, S., Kobayashi, O., Hatakeyama, K., Ushio, Y., Saya, H., and Hirota, T. (2003). CENP-A phosphorylation by Aurora-A in prophase is required for enrichment of Aurora-B at inner centromeres and for kinetochore function. Dev. Cell *5*, 853-864.

S6. Lenart, P., Petronczki, M., Steegmaier, M., Di Fiore, B., Lipp, J.J., Hoffmann, M., Rettig, W.J., Kraut, N., and Peters, J.M. (2007). The small-molecule inhibitor BI 2536 reveals novel insights into mitotic roles of polo-like kinase 1. Curr. Biol. *17*, 304-315.

S7. Schmitz, M.H., and Gerlich, D.W. (2009). Automated live microscopy to study mitotic gene function in fluorescent reporter cell lines. Methods Mol. Biol. *545*, 113-134.

S8. McHedlishvili, N., Wieser, S., Holtackers, R., Mouysset, J., Belwal, M., Amaro, A.C., and Meraldi, P. (2012). Kinetochores accelerate centrosome separation to ensure faithful chromosome segregation. J. Cell Sci. *125*, 906-918.

S9. Santaguida, S., and Musacchio, A. (2009). The life and miracles of kinetochores. EMBO J. *28*, 2511-2531.

S10. Gavet, O., and Pines, J. (2010). Progressive activation of CyclinB1-Cdk1 coordinates entry to mitosis. Dev. Cell *18*, 533-543.

S11. Held, M., Schmitz, M.H., Fischer, B., Walter, T., Neumann, B., Olma, M.H., Peter, M., Ellenberg, J., and Gerlich, D.W. (2010). CellCognition: time-resolved phenotype annotation in high-throughput live cell imaging. Nat. Methods *7*, 747-754.

S12. Taylor, S.S., Hussein, D., Wang, Y., Elderkin, S., and Morrow, C.J. (2001). Kinetochore localisation and phosphorylation of the mitotic checkpoint components Bub1 and BubR1 are differentially regulated by spindle events in human cells. J. Cell Sci. *114*, 4385-4395.

S13. Vink, M., Simonetta, M., Transidico, P., Ferrari, K., Mapelli, M., De Antoni, A., Massimiliano, L., Ciliberto, A., Faretta, M., Salmon, E.D., et al. (2006). In vitro FRAP identifies the minimal requirements for Mad2 kinetochore dynamics. Curr. Biol. *16*, 755-766.

S14. Jaqaman, K., King, E.M., Amaro, A.C., Winter, J.R., Dorn, J.F., Elliott, H.L., McHedlishvili, N., McClelland, S.E., Porter, I.M., Posch, M., et al. (2010). Kinetochore alignment within the metaphase plate is regulated by centromere stiffness and microtubule depolymerases. J. Cell Biol. *188*, 665-679.

S15. Schindelin, J., Arganda-Carreras, I., Frise, E., Kaynig, V., Longair, M., Pietzsch, T., Preibisch, S., Rueden, C., Saalfeld, S., Schmid, B., et al. (2012). Fiji: an open-source platform for biological-image analysis. Nat. Methods *9*, 676-682.